GEOFIZIKA VOL. 26 No. 2 2009

Original scientific paper
UDC 551.465

An operational system for forecasting hypoxic events in the northern Adriatic Sea

A. Russo[1,2], A. Coluccelli[1], I. Iermano[1,], F. Falcieri[1], M. Ravaioli[3], G. Bortoluzzi[3], P. Focaccia[3], G. Stanghellini[3], C.R. Ferrari[4], J. Chiggiato[5,**] and M. Deserti[5]*

[1] Polytechnic University of Marche – Dept. of Marine Science, Ancona, Italy

[2] National Research Council – Institute of Marine Science, Ancona, Italy

[3] National Research Council – Institute of Marine Science, Bologna, Italy

[4] ARPA Emilia-Romagna – Struttura Oceanografica "Daphne", Cesenatico, Italy

[5] ARPA Emilia-Romagna – Servizio Idro-Meteo-Clima, Bologna, Italy

Received 12 June 2009, in final form 10 December 2009

The northern Adriatic Sea (NA), the northernmost region of the Mediterranean Sea, is affected by strong anthropogenic pressure (e.g., tourism, fisheries, maritime traffic, discharge from agriculture and industry), superimposed to a large river runoff. The consequent pressure exerted on the NA ecosystem either triggers or worsens massive mucilage insurgence, harmful algal blooms, eutrophication and even anoxic/hypoxic events. This work focuses on the anoxic/hypoxic events. During the summer-autumn period, the NA is often exposed to these events, which can be categorised as either coastal (relatively frequent south of the Po River delta during the summer) and offshore (rare, affecting wider areas). In order to improve our knowledge about these processes and to meet the needs of local governments and decision makers, an operational system for monitoring and forecasting anoxic and hypoxic events has been set up in the framework of the EU LIFE "EMMA" project. The system is composed of a meteo-oceanographic buoy; a numerical prediction system based on the Regional Ocean Modelling System (ROMS), including a Fasham-type module for biogeochemical fluxes; and periodic oceanographic surveys. Every day since June 2007, the system provides 3-hourly forecasts of marine currents, thermohaline and biogeochemical fields for the incoming three days. The system has demonstrated its ability to produce accurate temperature forecasts and relatively good salinity and dissolved oxygen forecasts. The Root Mean Square Error of the dissolved oxygen forecast was largely due to the mean bias. The system is currently being improved to include a better

* Present address: Stazione Zoologica "Anton Dohrn", Napoli, Italy
** Present address: NATO Undersea Research Centre, La Spezia, Italy

representation of benthic layer biogeochemical processes and several adjustments of the model. While developing model improvements, dissolved oxygen forecasts were improved with the removal of the 10-day mean bias.

Keywords: anoxia, hypoxia, operational model, biogeochemical fluxes, Adriatic Sea, ROMS, marine forecast

1. Introduction

The northern Adriatic (NA) Sea is a marginal sea, bounded by the Italian peninsula to the West and by the Balkans to the East (Fig. 1). Due to the maximum latitude of its northern boundary (45° 47' N), it is the northernmost part of the Mediterranean Sea. Its bottom is very shallow, with an average bottom depth of approximately 35 m, and regularly and gently slopes southeastward until the 100 m isobath, arbitrarily taken as its southern open boundary. According to this definition, the southern boundary is approximately north of 43° 20' N (Artegiani et al., 1997a; Russo and Artegiani, 1996; Poulain et al., 2001). Other authors consider Ancona or Rimini to be the southern limit of the NA.

Being an epicontinental basin, the hydrology and dynamics of the NA are primarily influenced by meteorological forcing, thermal variations and river runoff. Climatological studies (see Cushman-Roisin et al., 2001 and citations therein) indicate that prominent weather situations in the NA include unperturbed weather or airflow from the northwestern, northeastern and southeastern quadrants (respectively Etesian, Bora and Sirocco winds). Bora and Sirocco are the most frequent winds in the area and often trigger severe windstorms. Despite its limited volume, the NA receives approximately 20 % of the total Mediterranean river runoff (Russo e Artegiani, 1996). This runoff comes mainly from the Po River, whose annual average flow rate is approximately 1500 m^3s^{-1} (Artegiani and Azzolini, 1981; Raicich, 1994). This leads to a net gain of fresh water (1.14 ± 0.20 m/year for the whole Adriatic Sea; Artegiani et al., 1997a; Russo and Artegiani, 1996). In autumn, intense cooling and evaporation processes, usually associated with Bora wind events over the NA, create conditions causing dense water formation during the winter (Vibilić and Supić, 2005). Due to runoff and heating in the late spring and summer and to autumn-winter cooling, gradient currents are established. This geostrophic response leads to a cyclonic circulation system (Zorè-Armanda, 1956; Buljan and Zorè-Armanda, 1976; Franco et al., 1982; Orlić et al., 1992; Artegiani et al., 1997a, 1997b; Russo and Artegiani, 1996; Hopkins et al., 1999; Poulain and Cushman-Roisin, 2001). This circulation pattern consists of an entering northwestward current (the Eastern Adriatic Current, EAC), which flows off of the eastern coast, and an exiting southeastward current (the Western Adriatic Current, WAC) off of the western coast. The former introduces warmer and saltier water into the sub-basin, while the latter delivers diluted water towards the southern regions. The general circulation pattern in the northern Adriatic is also largely affected by wind. For example, Bora episodes can gener-

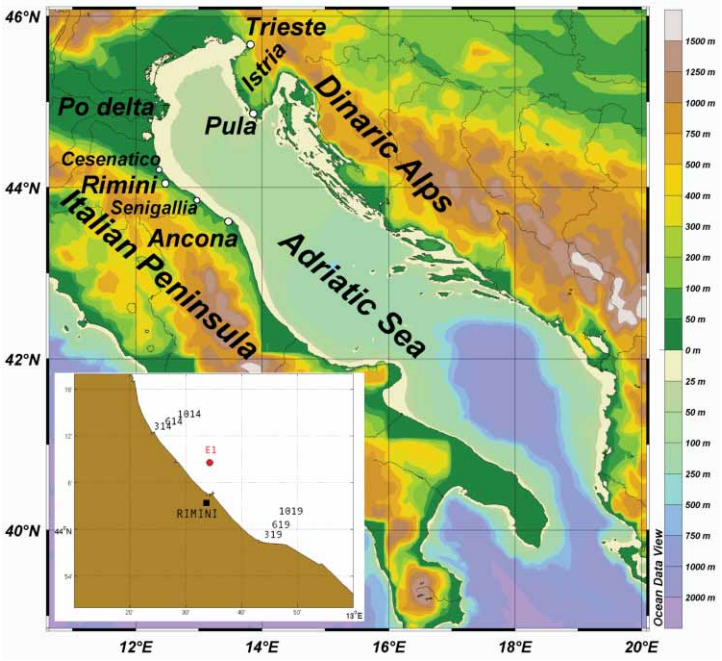

Figure 1. Study area and bathymetry; in the zoomed insert, the position of the E1 buoy position is shown, together with closest stations of ARPA Daphne monitoring.

ate a transient double gyre circulation consisting of a larger cyclone just north of the Po river delta and an anticyclone to the south, driving the upwind extension of Po River plume filaments (Jeffries and Lee, 2007). An anticyclonic circulation also develops along the southern Istrian coast (Poulain and Cushman-Roisin, 2001; Poulain et al., 2001), while Bora windstorms enforce flow in the WAC (Book et al., 2007; Ursella et al., 2007).

The NA Sea is one of the most biologically productive regions of the whole Mediterranean. The rate of oxygen consumption due to biogeochemical processes is the largest of the entire Adriatic basin, with a maximum occurring around the Po River delta area (Artegiani et al., 1997b). This region can thus be regarded as a favourable environment for the development of hypoxic conditions. The formation of a hypoxic bottom layer in wide areas of the watershed (Degobbis et al., 1993; Degobbis et al., 2000) can cause major ecological problems such as the mass mortality of marine animals, defaunation of benthic populations and a decline in fisheries production. Hypoxia is usually defined as occurring in regions where dissolved oxygen concentrations are less than 2 mL L^{-1} (equivalent to 2.8 mg L^{-1}). This concentration is the lower tolerance limit for many benthic species (Šimunović et al., 1999; Rabalais et al., 1999; Wu, 2002).

The occurrence of hypoxia and anoxia (no oxygen) can be associated with natural phenomena, such as vertical stratification caused by the formation of thermoclines and haloclines (Orel et al., 1986; Stachowitsch, 1986; Degobbis et al., 1993; Šimunović et al., 1999; Wu, 2002) which prevent the ventilation of the bottom layer. However, hypoxia and anoxia are nevertheless triggered by eutrophication, which is induced by nutrient inputs and enhanced by anthropogenic pressure. In fact, nutrients feed a high surface primary production and a consequent bottom decomposition of organic matter (Degobbis et al., 1993; Justić et al., 1995; Legović and Justić, 1997). According to Rabalais et al. (1999), the physics of the system defines where hypoxia can occur, while the biological factors lead to oxygen depletion.

During the colder seasons, the water column is generally well mixed and water exchange between the various parts of the Adriatic Sea is maximal. In the spring, the increasingly positive heat flux induces vertical stratification of density in the water column. Springtime high freshwater discharge in turn increases the surface layer buoyancy (Buljan and Zorè-Armanda, 1976; Artegiani and Azzolini, 1981; Franco et al., 1982; Orlić et al., 1992; Artegiani et al., 1997a; Russo and Artegiani, 1996). During the summer, a thermocline is generally observed at a depth of 10–30 m (Buljan and Zorè-Armanda, 1976; Artegiani et al., 1981; Russo and Artegiani, 1996). Thermal stratification confines riverine waters to the surface layer above the thermocline, and this allows for the wide horizontal distribution of such waters inside the basin (Artegiani et al., 1997b; Russo et al., 2002). Eventually, warm and fresh waters occur on top of cold and saltier bottom waters formed during the preceding winter, and strong vertical stability is reached.

In these situations, the bottom layer is almost isolated and gradually loses its oxygen content due to organic decomposition processes that occur on both sides of the water-sediment interface (Orel et al., 1986; Stachowitsch, 1986; Degobbis et al., 1993; Legović and Justić, 1997).

The influence of the Po River on hypoxic events is not only related to buoyancy input of freshwater, but also to its nutrient load, which can cause high surface productivity (Artegiani and Azzolini, 1981; Justić et al., 1995; Zavatarelli et al., 1998). According to Poulain et al. (2001), the Po River plume can be detected as the tongue of relatively fresh ($S < 35$), mesotrophic (chlorophyll *a* concentration > 1 μg/L) water. Dynamical stability and good light conditions limit nutrient dispersion and allow for massive phytoplankton blooms (Degobbis et al., 1993; Justić et al., 1995; Legović and Justić, 1997). Dead biomass sinks down to the bottom and degrades, coupling organic matter oxidation and nutrient mineralisation (Richards, 1965; Redfield et al., 1974; Orel et al., 1993). Under conditions of minimum water exchange, these processes can easily cause an increase in oxygen consumption (Orel et al., 1986; Stachowitsch, 1986; Degobbis et al., 1993).

As some authors pointed out (Justić et al., 1995; Legović and Justić, 1997), high turbidity related to the Po plume and to the high biomass production in

the surface layer can lead to the reduction of the euphotic depth due to decreasing light penetration. This in turn limits photosynthesis and oxygen production at depth. Thus, great organic matter sedimentation, resulting from increased pelagic primary production, contributes to oxygen depletion.

In the recent past (during 1977 and 1989), two major anoxic events have taken place over wide areas of the NA basin between the Po River delta and the Istrian Peninsula (Orel et al., 1993). Usually, anoxic events are much more frequent just south of the Po River delta during the warm season, but have a limited extension (Vollenweider et al., 1992; Orel et al., 1993).

The factors that play a major role in the development of hypoxic events in the northern Adriatic suggest that in principle it should be possible to establish an operational system able to provide detailed short-term forecasts of dissolved oxygen changes in the basin. Similar systems have been established in other areas such as the Gulf of Mexico (see the review by Justić et al, 2007 and citations therein).

Beginning in the last decade of the twentieth century, much effort has been made to promote and sustain the development of operational ocean forecasting systems, which are considered essential to the management, protection and exploitation of coastal environments. Operational oceanography of the Mediterranean Sea is now approaching a mature stage with the proliferation of several regional forecasting systems (for currents, thermohaline fields, sea level, waves) nested in large-scale systems (e.g., the Mediterranean Forecasting System, MFS; Pinardi et al., 2003, Tonani et al, 2008). Within the framework of the MFS, a biogeochemical flux model (based on the BFM model; Vichi et al., 2007) has been providing an operational forecast of nutrients, chlorophyll, phytoplankton and zooplankton since May 2007 over the whole Mediterranean Sea at a 1/8° (approximately 14 km) horizontal resolution. This system is coupled offline with the physical MFS model. In the Adriatic Sea, several hydrodynamic models have successfully simulated the mesoscale variability of the basin (e.g., Martin et al, 2006; Cushman-Roisin et al., 2007). Regional systems, such as the Adriatic REGional model (AREG; Oddo et al., 2006) and the Adriatic implementation of the Regional Ocean Modeling System (AdriaROMS; Chiggiato and Oddo, 2008), have now been operational for several years, but they do not provide forecasts for hypoxic events and are not yet coupled with biogeochemical components.

The present work focuses on the operational system for the observation, monitoring and short-term forecast of hypoxic events in the Romagna coastal area (south of the Po River Delta). The system has been implemented within the framework of the "Environmental Management through Monitoring and Modelling of Anoxia" (EMMA) project, which was funded by the EU LIFE program. The EMMA operational system is composed of a meteo-oceanographic buoy and a hydrodynamic numerical model (including a biogeochemical module) that is forced by a limited area numerical weather prediction model; periodic oceanographic surveys complement the system. Hereafter, numerical mo-

dels are described together with the *in situ* measurements, and then the model vs. data comparisons are shown. Performances of the system and possible improvements are discussed and final conclusions are drawn.

2. Materials and methods

2.1. In situ measurements

Within the framework of the EMMA project, the meteo-oceanographic buoy E1 was deployed (and it is being managed) by ISMAR-CNR (Bologna) on the 9th of August, 2006, approximately 6 km offshore from Rimini (Fig. 1) on a bottom depth of 10.5 m. The buoy was equipped with meteorological sensors manufactured by Aanderaa Data Instruments AS for air temperature, air pressure, wind speed and gusts, wind direction, relative humidity, and net solar radiation. Oceanographic sensors are positioned at two levels. The first level, at approximately 1.6 m below the sea surface, has pressure, temperature and conductivity sensors manufactured by Sea Bird Electronics Inc.; the same sensors are located on the bottom level (at approximately 8.4 m depth, 2.1 m above seafloor), plus a SBE 43 dissolved oxygen sensor and an Aanderaa DCS–3900 single point current sensor. Data were recorded every 15–30 min and transmitted to ISMAR–CNR (Bologna) through mobile phone and internet connections at intervals between one and three hours (the latter in the case of long-lasting fog reducing the charging capabilities of solar panels).

During an EMMA oceanographic cruise conducted in the NA from the 21st to the 24th of May, 2007 onboard the R/V Dallaporta of CNR–ISMAR, 123 CTD vertical profiles were collected. At each oceanographic station, a CTD probe was lowered from the sea surface to a depth of approximately 1 m above the sea bottom. The CTD probe used was a Sea Bird Electronics SBE 911plus, equipped with calibrated pressure, temperature, conductivity and dissolved oxygen (SBE 43) sensors, as well as other ancillary sensors. CTD data were processed according to standard procedures, while derived variables (salinity, density) were computed and final averages were produced in 0.5 m vertical bins. Temperature, salinity and dissolved oxygen values acquired during this cruise were used to initialise the ROMS model as discussed below.

The "Daphne II" vessel of the ARPA–SO Daphne (Cesenatico, Italy) used similar procedures during its regular monitoring (occurring monthly, and biweekly during the summer period) of the Emilia-Romagna Region coastal area. In this case, the CTD probe used was an Idronaut Ocean Seven 316 with calibrated sensors for pressure, temperature, conductivity and dissolved oxygen, as well as other ancillary sensors. The processed data were made available until the end of the EMMA project (September 2007).

Po River runoff data were measured by the Hydro-Meteo-Clima service of the ARPA – Emilia Romagna Region (Bologna, Italy) at the Pontelagoscuro site (approximately 80 Km inland, just before the delta ramification).

2.2. Description of the numerical models

The core ocean model is the Regional Ocean Modelling System (ROMS, http://www.myroms.org; Shchepetkin and McWilliams, 2005; Haidvogel et al., 2008). It is a primitive equation, finite difference, hydrostatic, free surface model that uses generalised terrain following *s*-coordinates and staggered Arakawa C grid on the horizontal and split-explicit, non-homogeneous predictor/corrector time steps.

The Adriatic application has been configured on an orthogonal curvilinear grid, with a constant resolution of 2 km across the entire domain, and 20 vertical *s*-levels, which have been conveniently stretched to allow for a higher resolution of the surface and bottom boundary layers.

The advection of tracers is integrated using a recursive MPDATA (Multidimensional Positive Definite Advection Transport Algorithm) family scheme (Margolin and Smolarkiewicz, 1998). A weak grid-size dependent, harmonic form (Laplacian) horizontal diffusivity is applied, while no horizontal viscosity is added. The pressure gradient term was made discrete by means of a density Jacobian with cubic polynomial fits (see Shchepetkin and McWilliams, 2003). Parameterisation of vertical mixing followed the Mellor/Yamada level 2.5 turbulence closure scheme (Mellor and Yamada, 1982).

Tidal elevation and currents for the main tidal components (M2, S2, K1, O1) were imposed along the southern open boundary (Otranto Strait area) with values resulting from a finite-element model of the whole Mediterranean (Cushman-Roisin and Naimie, 2002). The barotropic field boundary conditions were prescribed according to Flather (1976) for the 2–D momentum and Chapman (1985) for the tidal elevation. A radiation boundary condition (Marchesiello et al, 2001) was used for baroclinic fields and tracers.

Forty-eight rivers and Carsic springs (in the Croatian area) were also included as sources of mass, momentum and nitrate using available daily discharges for the Po River or monthly climatological values (Raicich, 1994) when daily data was not available. Thirteen additional sources were placed along the Emilia Romagna coast in order to simulate the higher release of nutrients from urban discharges, particularly those caused by the presence of large numbers of tourists during the summer.

Fluxes through the air-sea interface were calculated using the COARE 3.0 bulk flux algorithms (Fairall et al., 2003) with sea surface temperatures (SST) calculated from ROMS and short wave radiation, wind, air temperature, humidity, cloud cover and atmospheric pressure provided from the COSMO–I7 atmospheric model. COSMO–I7 (formerly LAMI), a local implementation of the Lokall Model (LM; Steppeler et al., 2003), is a non-hydrostatic numerical weather prediction model with a 7 km horizontal resolution that provides hourly outputs with a 72-hour forecast range released twice a day (00 – 12 UTC). The COSMO model is managed by the ARPA–EMR–SIMC, by the

USAM (Ufficio Generale Spazio Aperto e Meteorologia of the Italian Air Force) and by the ARPA Piemonte.

The ROMS model is the result of a long history of development within the terrain-following ocean modelling community; nowadays, this model is considered to be a multi-disciplinary and multi-purpose marine modelling tool. This model incorporates expertise from a wide variety of problem classes; one of the most interesting being the investigation of biogeochemical cycles and ecosystem dynamics. ROMS offers a range of ecological sub-models; in order to simulate biogeochemical fluxes including dissolved oxygen, we used the Fasham--type biological module (Fennel et al., 2006), renamed the Fennel module beginning at the release of the ROMS version 3.2.

The Fennel module is a modified version of Fasham's model (Fasham et al., 1990); it reproduces pelagic nitrogen cycle processes in the water column and remineralisation processes at the water-sediment interface, explicitly taking into account denitrification and sediment processes to restore sunken particulate material in the nutrient pool. In addition, the Fennel module simulates inorganic carbon and dissolved oxygen dynamics. The inorganic nitrogen species nitrate and ammonium are treated as separate state variables, while chlorophyll is included as a prognostic variable in addition to phytoplankton and zooplankton biomass. Two size-classes of detritus are considered to allow for different settling rates (small detritus $S_{det} < 10\ \mu m$ and large detritus $L_{det} = S_{det} + Phyt$) and are expressed in terms of nitrogen and carbon concentrations.

A long simulation of the ROMS with the Fennel module in the Adriatic Sea ran for a time period of five years (Iermano, 2008). This implementation was used to investigate and define the model setup for the EMMA application and provides initial conditions for some biogeochemical variables. An additional, analytical negative flux of dissolved oxygen at the bottom was necessary in order to account for limitations due to model-simplified benthic processes. The sediment component of the Fennel model included in ROMS is a relatively simple representation of benthic mineralisation processes, i.e., the remineralisation of deposited organic matter on top of the sediment is formulated as a bottom boundary condition (Fennel et al, 2006). A negative constant flux of 0.115 $\mu mol\ m\ s^{-1}$ of dissolved oxygen at the bottom (derived from the literature considering sediment oxygen consumption in the Adriatic Sea, e.g., Moodley et al., 1998, and by sensitivity studies) was added into our model.

The operational version of ROMS described in this work has been implemented and is being managed at the Department of Marine Science at Polytechnic University of Marche (Ancona, Italy). The model was initialised using an averaged field output of a diagnostic run in which temperature and salinity were held constant in order to lower the spin-up time. Such temperature and salinity fields originally came from objective analysis mapping of data collected during the May 2007 synoptic cruise (described in the previous section) combined with climatologic data (MEDAR Group, 2002) for the southern part

of the Adriatic basin. Also, the dissolved oxygen 3–D field was obtained by combining data measured during the synoptic cruise in the NA and climatological values elsewhere. The other biogeochemical variables were initialised by interpolating the output of the long-term simulation (5 years) conducted in the Adriatic Sea with a coarser resolution ROMS grid (Iermano, 2008).

Starting at the end of May 2007, a daily automated procedure downloads COSMO–I7 surface forecasts and Po River runoff data from a dedicated FTP site at ARPA–EMR–SIMC every day and processes these data to produce the files needed for the ROMS run, that produces forecasts for 72 hours. At present, the forecast of the Po River runoff is not operational, so the current Po River runoff is kept constant during the run. Each ROMS forecast is initialised by a restart file produced by the ROMS run of the day before. At the end of the ROMS run, the output is post-processed in order to produce specific products (e.g., dissolved oxygen and related fields in the EMMA project area of interest).

3. Results

The EMMA operational system has provided real-time data (E1 buoy) and forecasts (ROMS model with biogeochemical module) continuously since August 2006 and June 2007, respectively. Time series of raw data provided by the buoy and the corresponding output of model forecasts are shown (no filter or special processing has been applied) in Figures 2–5. Five minute data averages and corresponding instantaneous model outputs at three-hour intervals were used for temperature, salinity and dissolved oxygen values, whereas daily averages of current speed were compared because of the higher variability of this factor (due, for example, to tides).

The surface layer temperature (at a depth of 1.6 m) is presented in Figure 2.a. Minimum values of approximately 6 °C were recorded in January 2007 and 2008. Surface heating began at the end of February, with temperatures reaching values above 25 °C (up to 28 °C in 2008) in July and August of both years; some cooling was evident during July 2007, with temperatures of less than 25° C being observed for a few weeks. The period of autumn cooling began at beginning of September in 2007 (with a temperature drop of approximately 5 °C in roughly one week) and in mid-September of 2008 (with a temperature drop of almost 10 °C in a roughly two weeks). The temperature forecasted by the model (in blue) closely follows the temperature recorded by the buoy, showing good forecasting capabilities in the surface layer. The Root Mean Square Error (RMSE) of the model forecast was 0.90 °C over the whole period, with a minimum of 0.65 °C in the summer and a maximum of 1.02 °C in the winter season. The correlation between the measured and forecasted temperature was very high (0.993).

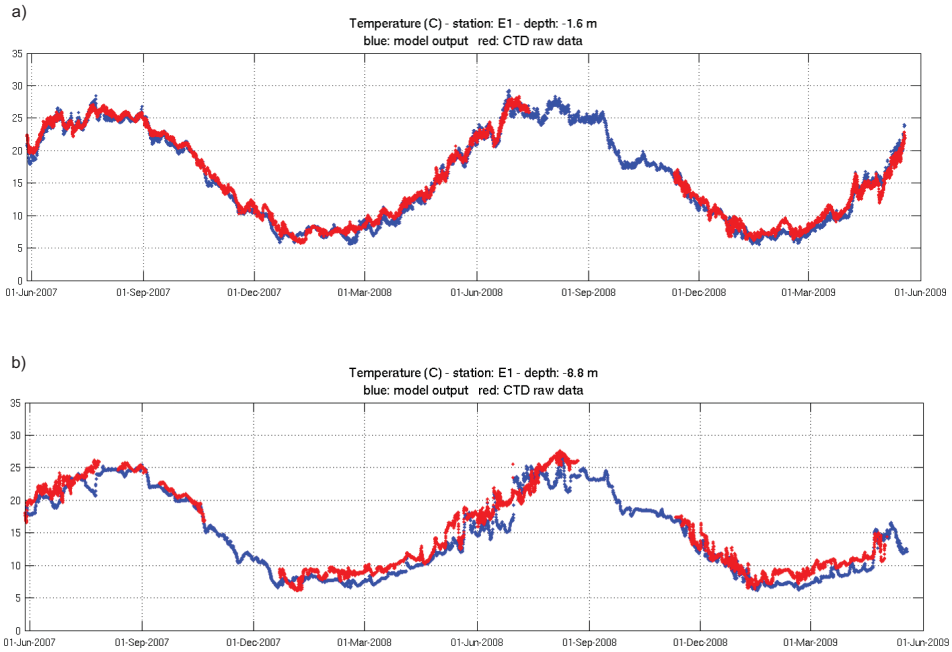

Figure 2. Time series of: a) surface (1.6 m depth); and b) bottom layer (8.8 m depth, 1.5 m above seafloor) temperature (°C) from June 2007 to May 2009; buoy data are shown in red, model forecasts are in blue.

The bottom layer temperature (at 8.8 m depth) is presented in Figure 2.b. Temperature minima were reached at beginning of January 2008 and in January 2009, with values below 7 °C. Maxima were reached at the beginning of August 2008 and August 2007, with values of over 25 °C. The cooling period in both 2007 and 2008 began in September with a fairly abrupt drop of several degrees centigrade (approximately 7 degrees in 2008 and 3 degrees in 2007). This cooling continued until the January minimum, at which point the temperature stabilised at approximately 7–8 °C until March when the heating period began. A sudden increase of several degrees centigrade was observed in mid-May 2008 and in the beginning of May, 2009. The model is able to forecast changes in the bottom layer temperature reasonably well; nevertheless the observed temperature was often underestimated. The best model performances were obtained in the first part of the period (summer-autumn 2007) and from November, 2008 until January, 2009. The RMSE was almost double that of the surface, with an average value of 1.77 °C over the whole period, a minimum value of 0.98 °C during the autumn and a maximum value of 2.10 °C during the spring season. Instead, the correlation between the measured and forecasted temperatures remains very high (0.976).

Surface salinity (Fig. 3.a) shows a higher variability than temperature, with little evidence for a seasonal signal. However, a high salinity variability related to Po River runoff was observed at higher and lower (interannual) frequencies. The minimum salinity values were very low (below 25) and were reached only after one year of observations, in June 2008, and again in the winter of 2008–09 and the spring of 2009. Salinity values remained higher (often above 35, which is a quite a high value for this area) in the first year of observation than in the second year, reflecting the Po River runoff. The Po River runoff was always well below the climatologic monthly average during the first year, while in June 2008 it reached a value that was almost twice the average. In the autumn, the runoff was again well below the average, while runoff was above the average in 2009. Periods of minimum salinity values reflected peaks in the Po River runoff. Surface salinity forecasts reflected the observed salinity variations relatively well, showing generally higher values during the first year and closer values during the second year. The large variability of salinity values is reflected in the RMSE of the model forecast, which has an average value of 2.21 with a maximum value of 2.55 in the autumn and a minimum value of 1.34 in the summer. The correlation between measured and forecasted salinity is fairly good (0.733).

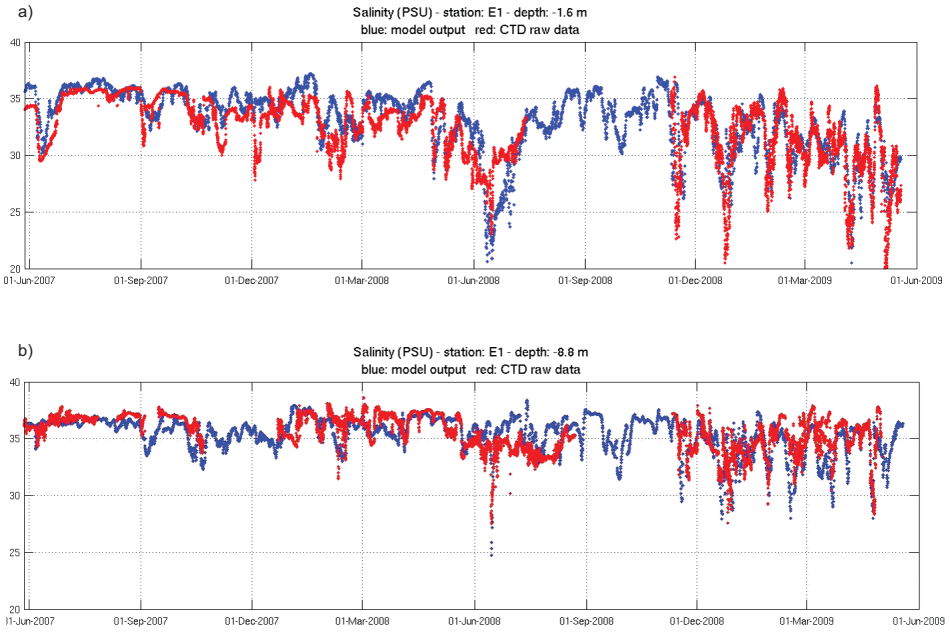

Figure 3. Time series of: a) surface (1.6 m depth); and b) bottom layer (8.8 m depth, 1.5 m above seafloor) salinity from June 2007 to May 2009; buoy data are shown in red, model forecasts are shown in blue.

Salinity in the bottom layer (Fig. 3.b) showed relatively higher values compared to the surface salinity values, although showing a similar general trend given the site shallow depth (8.8 m). In fact, the buoy recorded lower salinities and a higher variability in salinity values during the second year, with the only exception of the less evident decrease in salinity in June–July 2008. This suggests that a shallow thermocline confined freshwater to the uppermost surface layer. Minimum salinity values were observed at the bottom and at the surface in the very same periods, but the bottom salinity was approximately 5 units greater with minimum values lasting for shorter periods. Model forecasts represent the salinity evolution fairly well most of the time. However, the model performed better in some periods. The RMSE for bottom salinity was better than the RMSE at the surface because of the lower variability: the average RMSE was 1.55 for the whole period, with a maximum of 1.79 in the winter and a minimum of 1.22 in spring. However, the correlation was worse for salinity at bottom, with a value of only 0.554.

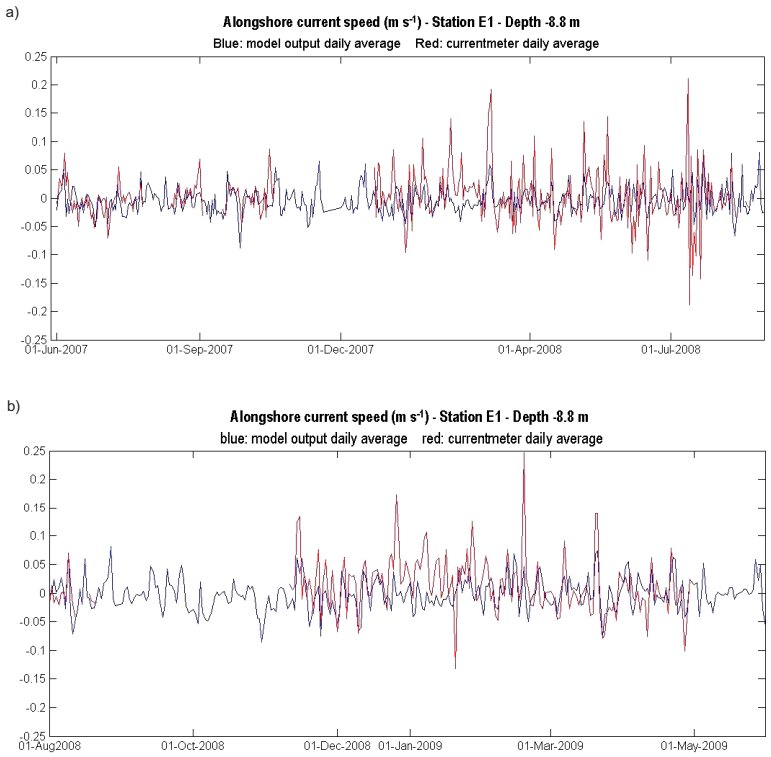

Figure 4. Time series of daily averaged alongshore current speed (m s^{-1}, positive toward southeast) in the bottom layer (8.8 m depth, 1.5 m above seafloor) for: a) the period from the 1st of June, 2007, until 31st of July, 2008; and b) the period from the 1st of August, 2008 until the 30th of May, 2009; buoy data are shown in red, model forecasts are shown in blue.

Bottom currents are relevant to the development of hypoxia as they can enhance or reduce hypoxic events by means of the advection of waters that are either poor or rich in dissolved oxygen; hypoxic waters that may reach the Rimini area mainly flow parallel to the coast from the Po River Delta area (i.e., from the northwest). Fig. 4 shows the alongshore component of the bottom layer currents (positive values indicate southeast currents). The model correctly forecasted the current speed during several periods, while at other times the predicted direction of the current was incorrect. Generally, the forecasted bottom currents appeared to be underestimated, with a constant monthly mean bias of approximately –0.05 m s^{-1} throughout the entire period. The RMSE remained at approximately 0.1 m s^{-1}, except in July 2008 when it doubled. In July, 2008, the highest currents of the entire periods were recorded by the E1 buoy current meter, whilst the model did not show any anomalous patterns. During this period, the E1 buoy was found to be heavily biofouled, which modified its buoyancy and very likely affected the current measurements.

Dissolved oxygen (Fig. 5) was recorded at the E1 buoy in the bottom layer (8.8 m depth) only. Minimum values of less than 2 mL L^{-1} indicated hypoxia and were reached in June–August 2008 in response to the marked increase in the June Po River runoff (though it should be noted that during July 2008, biofouling accumulated on the sensor and the data from this time period were thus not fully reliable). The model was able to forecast the general cycle of dissolved oxygen at the bottom during the entire study period, though the model performance was variable (the model performed quite well during the first months, but less well after the spring of 2008). The RMSE was 1.67 mL L^{-1} over the two years, with a maximum value of 1.92 mL L^{-1} in the autumn and a minimum value of 1.34 mL L^{-1} during the spring season. The correlation between the measured and forecasted dissolved oxygen values was relatively good (0.730).

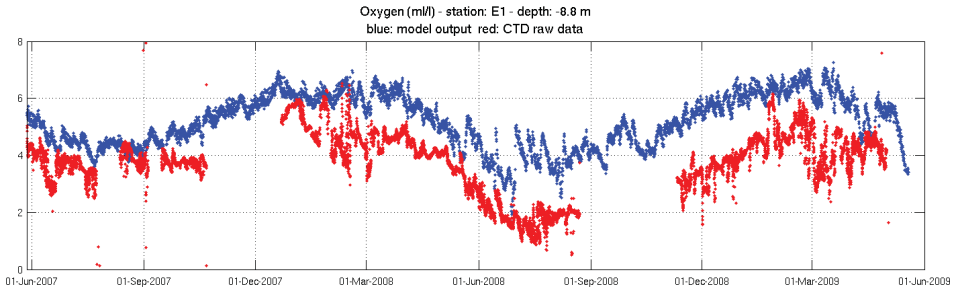

Figure 5. Time series of the bottom layer (8.8 m depth, 1.5 m above seafloor) dissolved oxygen (mL L^{-1}) from June 2007 to May 2009; buoy data are shown in red, model forecasts are shown in blue.

A more detailed quantitative analysis of the model performance can be conducted using several approaches. For example, the Mean Square Error (MSE) can be used as follows: MSE = $\langle(m_i - o_i)^2\rangle$, where m_i = modelled values and o_i = observed values. According to Murphy (1992) and Oke et al. (2002), the MSE comprises contributions from the mean bias, MB = $\langle m\rangle - \langle o\rangle$, the standard deviation error, SDE = $S_m - S_o$, and the cross-correlation:

$$\mathrm{CC} = \mathrm{S}_m^{-1}\, S_o^{-1} \langle(m_i - \langle m\rangle)\, \langle(o_i - \langle o\rangle)\rangle,$$
$$\text{being } \mathrm{RMSE}^2 = \mathrm{MB}^2 + \mathrm{SDE}^2 + 2\, S_m^{-1}\, S_o^{-1}\, (1\text{–CC})$$

where S_m and S_o are the respective modelled and observed standard deviations. This approach has been already used for the evaluation of the ROMS skill (e.g., Wilkin et al., 2006). Results of the MSE analysis of dissolved oxygen measured by the E1 buoy and the corresponding modelled values are shown in Fig. 6. It is evident that monthly RMSE values were dominated by MB, which showed an initial increase and then appeared to stabilise during 2008 and 2009. The SDE, or amplitude error, indicates that the forecast had a feasible variability, with the exception of the late winter – early spring period when the modelled data showed less variability than measured data. The monthly correlation between the measured and forecasted dissolved oxygen was not high, and also showed negative values in August, September and December 2007.

In order to extend the area of comparison and to provide an independent marine dataset, we considered the stations monitored bimonthly by ARPA Daphne during the EMMA project (ended in September 2007) that were closest to the E1 buoy (locations indicated in the insert of Fig. 1). Fig. 7 shows the

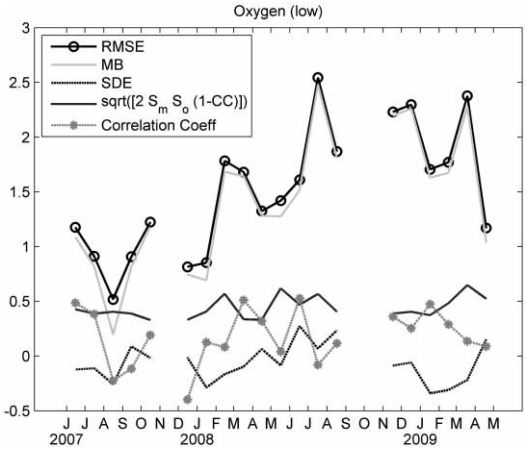

Figure 6. Monthly values of model-data error terms for dissolved oxygen at the bottom level of the E1 Buoy.

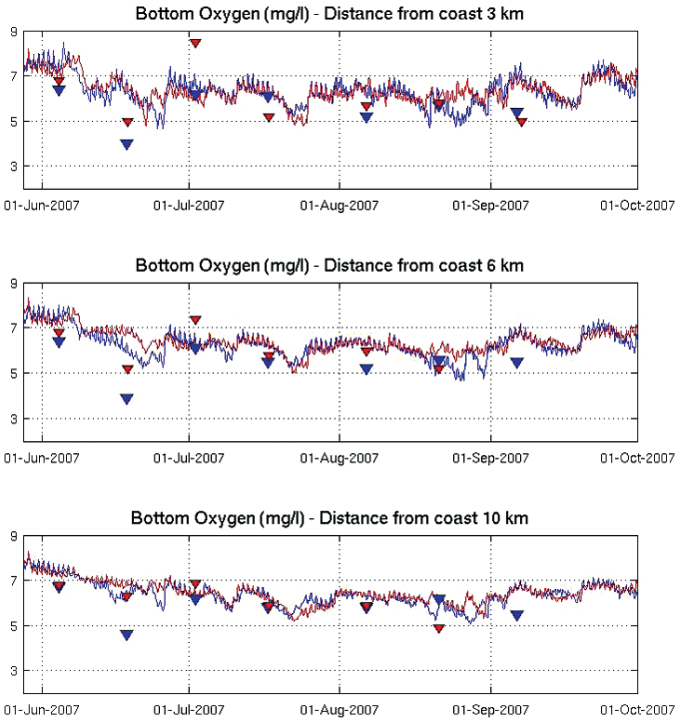

Figure 7. Time series of forecasted bottom layer dissolved oxygen (mg L^{-1}) at ARPA–Daphne stations 314 and 319, 614 and 619, 1014 and 1019, located 3, 6 and 10 km from the coast, respectively (Fig. 1), from June to September 2007; triangles indicate the corresponding values of dissolved oxygen measured by ARPA–Daphne (blue shows the stations of transect 14, while red indicates the stations of transect 19).

forecasted bottom dissolved oxygen values (in mg L^{-1}) with *in situ* values measured along two transects, north and south of the E1 buoy. The measured data in the two transects showed a similar trend, except for a quite anomalous higher value at station 319 at the beginning of July 2007 (Fig. 7). The coastal and very shallow stations located 3 and 6 km from the coast showed a relevant variability on both transects, while the offshore (10 km from the coast) stations showed more limited variability. The model forecast presented the same behaviour, with variability decreasing from the coastal to the offshore stations. The forecast accuracy appeared to be better for the offshore stations.

4. Discussion

The EMMA system was found to be a reliable tool providing data and forecasts in the Rimini area continuously. Since it can be likely to have interrup-

tion of data flow from an oceanographic buoy because of many problems that can arise (e.g. a lack of connectivity, hardware failure, biofouling, accidents, etc.), the availability of an operational model is useful for reducing the consequences of a temporary lack of buoy data. Forecasts provided by the model demonstrated a good performance as far as temperature, whereas the performance for predicting both salinity and dissolved oxygen was not as strong.

The dissolved oxygen weaker performance was expected because of the several limitations of the biogeochemical module, that were thought to be responsible for the overestimations of the model evident in Fig. 5. The dissolved oxygen flux at the seafloor is over-simplified, resulting from immediate remineralisation of detritus, and from a constant sink term introduced to take neglected processes into account. The Fennel module was designed for the US eastern continental shelf and there are several differences between this system and a coastal system such as the NA Sea (e.g., only nitrogen is considered to be limiting nutrient, whereas in NA phosphorus can be limiting nutrient in some periods and areas; light penetration is strongly reduced in areas affected by the turbid Po River plume, an effect that is still not included in the model, which considers only self-shading). In addition, nitrogen concentration of the Po River waters were based on literature data, but Po River runoff changed during the last years, and changes in nutrient concentration may also have occurred. For other rivers, and particularly the rivers of the Emilia-Romagna region, real-time runoff data were not available so monthly climatological values were used; considering that nutrient concentration data were often not available, the riverine input of water and nutrients is rather inaccurate, as is the nutrient input from the coast. Moreover, the sink term of dissolved oxygen in the bottom layer that was introduced into the model was kept constant in space and time at a value (0.115 μmol m s^{-1}, or 414 μmol m h^{-1}) that is quite close to the annual NA basin average, however underestimating the real values observed in the Rimini area (which are 2–3 times greater, with maximum values observed during the warm season; e.g., Moodley et al., 1998). The sediment component of the Fasham-type model included in the ROMS is a relatively simple representation of benthic mineralisation processes, with remineralisation of deposited organic matter on the top of the sediment being formulated as a bottom boundary condition (Fennel et al, 2006). This implies that in the model the flux of sinking organic matter outward of the deeper grid box results in a corresponding inward flux of inorganic nutrients at the sediment/water interface. In the classification of benthic-pelagic coupling formulations given by Soetaert et al. (2000), this approach is considered to be of intermediate complexity (a formulation of mass conservation assuming the immediate balance between particle deposition and the flux of dissolved constituents returned from the sediment). Soetaert et al. (2000) show that this approach is efficient from a computational point of view, and that accounts for a large portion of the dynamics inherent in benthic-pelagic coupling. Considerations of a delayed coupling (the accumulation of deposited organic matter coupled with a

temperature-dependent decomposition) would require a computationally more expensive diagenetic model, which we are currently defining. The current operational implementation was based on the consideration that in most situations in marine ecology, physical processes are the primary determinants of the dynamics of marine ecosystems: "In estuaries, on continental shelves and in the open ocean, the physical processes appear to set the stage on which the biological play is enacted" (Mann and Lazier, 1991). So, when "simple" biological models are used in conjunction with an accurate representation of abiotic factors (driven by hydrodynamic processes in high resolution), or rather coupled with sophisticated hydrodynamic numerical models (as ROMS model), they are capable of describing a large part of the system observed.

The hydrodynamics forecasted by ROMS are important to the diffusion and advection of dissolved oxygen in the water column. Comparisons with buoy data demonstrated the model's ability to accurately forecast the surface temperature; temperature close to the bottom (at approximately 9 m) showed a more evident deviation from observed values but still maintained a very high correlation with the observed values. The forecast accuracy appeared to be lower for bottom layer currents and much lower for salinity values, particularly at the bottom. It should be noted that a punctual comparison is very difficult in this very shallow water (10.5 m bottom depth) and, especially during the warm period, an uncertainty of tenths of centimetres in the depth sensors may result in important differences in temperature and salinity (as well as dissolved oxygen). Interestingly, the best performances of the model were obtained in the summer for surface temperatures and in the autumn for bottom temperatures, while the worst performance was observed in the winter for surface temperatures and in the spring for bottom temperatures. This could be related to a lack in the model implementation of measured Po River water temperatures. In fact, waters entering from the Po River alter the sea temperature, particularly during the winter period around the Po River Delta and in the coastal area south of the delta. The model used mean values deduced by Po temperature time series acquired during 2002–03. The comparison with the buoy data, particularly in the case of salinity, depicts the skill of the system to forecast the main trend, but with some evident deviations. However, the E1 buoy, located nearshore (less than 6 km offshore Rimini, with a model horizontal resolution of 2 km), can be affected by runoff from both the Po River and from local rivers and real values of the other rivers were not included. Forecasts of the bottom currents appear to underestimate the measured values at the E1 buoy in several cases; in quite shallow waters (approximately 10 m depth), these currents could have important effects through waves-current interactions, which were not considered in the present model. For these reasons, improvements in forecasting hypoxia in addition to the biogeochemical flux module could be acquired also in other ways, e.g., by increasing the resolution and improving the turbulence parameterisation, air-sea fluxes, boundary conditions at the Otranto Straits (deducing them from AREG or MFS sys-

tem), runoff from minor rivers, by coupling with a wave model, by the timely (preferably once a year in spring) re-initialisation from data measured during synoptic surveys in the NA.

One positive aspect of this model is the fact that most of the dissolved oxygen RMSE was due to the MB (Fig. 6). This implies that the variability of the processes was simulated correctly and the bias can be reduced by applying data assimilation techniques and by using post processing. Understanding and solving the problems of this bias would improve the forecast skill of the model.

We are currently working to improve the ROMS operational implementation with regards to the aspects of the model discussed above. Meanwhile, the dissolved oxygen forecast is currently being corrected by the MB calculated over a 10 day period.

5. Conclusions

A number of different simulation and statistical models have been used to nowcast, hindcast, and forecast the severity and areal extent of hypoxia in certain areas of the world, such as the northern Gulf of Mexico (Justić et al., 2007). In particular, Hetland and DiMarco (2007) modelled the Texas-Louisiana shelf using the ROMS model with a parameterisation of biological activity through various simple respiration models, rather than a biogeochemical flux model such as that used in our implementation. Results indicate that water column respiration reproduces the observed temporal and spatial structure of hypoxia in the vicinity of the Mississippi River Delta, while the benthic respiration seems to be the predominant oxygen sink in the remaining area experiencing hypoxia. The formation and breakdown of hypoxia in the Gulf of Mexico results primarily from vertical processes and it appears that hypoxic waters formed in one region are not advected to other shelf regions. This Gulf of Mexico ROMS implementation has been used for process studies and not for operational forecasts. To the best of our knowledge, the EMMA system is probably the first system that is able to produce operational 3–D short-term forecasts of hypoxia in the Mediterranean area. Analysis of results and data comparison showed the sustained capability both to monitor and to operationally forecast hypoxia in the Rimini area in the short-term. In particular, despite the absence of any kind of data assimilation and the very simple biogeochemical module, the ROMS model has been able to forecast the dissolved oxygen in Rimini and the wider Emilia-Romagna coastal area with a reasonable degree of approximation for almost two years of continuous integration. It is however clear that, in order to produce more reliable forecasts of dissolved oxygen and other marine properties, the model would benefit from several improvements, which are currently being developed.

Acknowledgements – The support of the EU LIFE program (contract LIFE04 ENV/IT/000479) is gratefully acknowledged. Some activities were also supported by the Ital-

ian Ministry for University and Research though the FIRB program (ANOCSIA project) and by the Emilia-Romagna Region.

We wish to thank the captains, crew and personnel onboard the R/V Dallaporta (CNR) and R/V Daphne (ARPA Emilia Romagna) for their fundamental support during *in situ* data collection. We also wish to thank Dr. Elio Paschini (ISMAR–CNR, Ancona) for making the SBE 911plus CTD probe available during the R/V Dallaporta cruise. Italian Coast Guard and volunteers of the "Volontari Soccorso in Mare" of Rimini (Italy) provide important help in the maintenance of the E1 buoy. We are also grateful to the two anonymous referees whose comments improved the quality of the manuscript.

References

Artegiani, A. and Azzolini, R. (1981): Influence of the Po floods on the western Adriatic coastal water up to Ancona and beyond, *Rapp. Comm. int. Mer Médit.*, **27**(6), 115–119.

Artegiani, A., Bregant, D., Paschini, E., Pinardi, N., Raicich, F. and Russo, A. (1997a): The Adriatic Sea general circulation. Part I: Air-sea interactions and water mass structure, *J. Phys. Oceanogr.*, **27**(8), 1492–1514.

Artegiani, A., Bregant, D., Paschini, E., Pinardi, N., Raicich, F. and Russo, A. (1997b): The Adriatic Sea general circulation. Part II: Baroclinic circulation structure, *J. Phys. Oceanogr.*, **27**(8), 1515–1532.

Book, J.W., Signell, R.P. and Perkins, H. (2007): Measurements of storm and nonstorm circulation in the northern Adriatic: October 2002 Through April 2003, *J. Geophys. Res.*, **112**, C11S92, DOI:10.1029/2006JC003556.

Buljan, M. and Zore-Armanda, M. (1976): Oceanographical properties of the Adriatic Sea, *Oceanogr. Mar. Biol. Ann. Rev.*, **14**, 11–98.

Chapman D.C. (1985): Numerical treatment of cross-shelf open boundaries in a barotropic coastal ocean model. *J. Phys. Oceanogr.*, **15**, 1060–1075.

Chiggiato, J. and Oddo, P. (2008): Operational ocean models in the Adriatic Sea: a skill assessment, *Ocean Sci.* **4**, 61–71.

Cushman-Roisin, B., Gačić, M., Poulain, P.-M. and Artegiani, A. (2001): *Physical Oceanography of the Adriatic Sea: Past, Present and Future*, Kluwer Acad., Norwell, 304 pp.

Cushman-Roisin, B. and Naimie, C. E. (2002): A 3D finite-element model of the Adriatic tides, *J. Marine Syst.*, **37**, 279–297.

Cushman-Roisin, B., Korotenko, K.A., Galos, C.E. and Dietrich, D.E. (2007): Mesoscale resolving simulations of the Adriatic Sea Variability, *J. Geophys. Res.*, **112**, C03S14, DOI:10.1029/2006JC003515.

Degobbis, D., Travizi, A. and Jaklin, A. (1993): Meccanismi di formazione di strati di fondo ipossici e anossici nel bacino dell'Alto Adriatico settentrionale e reazioni delle comunità bentoniche, in *Ipossie e anossie di fondali marini. L'Alto Adriatico e il Golfo di Trieste*, edited by Orel, G., Fonda Umani, S. and Aleffi, F., Regione autonoma Friuli Venezia Giulia, Direzione regionale dell'Ambiente, Trieste, Italy. (in Italian).

Degobbis, D., Precali, R., Ivancic, I., Smodlaka, N., Fuks, D. and Kveder, S. (2000): Long-term changes in the northern Adriatic ecosystem related to anthropogenic eutrophication, *Int. J. Environ. Pollut,*, **13**(1–6), 495–533.

Fairall, C.W., Bradley, E.F., Hare, J.E., Grachev, A.A. and Edson, J.B. (2003): Bulk parameterisations of air-sea fluxes: updates and verification for the COARE algorithm, *J. Climate*, **16**, 571–591.

Fasham, M.J.R., Ducklow, H.W. and McKelvie, S.M. (1990), A nitrogenbased model of plankton dynamics in the oceanic mixed layer, *J. Mar. Res.,* **48**, 591– 639.

Fennel, K., Wilkin, J., Levin, J., Moisan, J., O'Reilly, J. and Haidvogel, D. (2006): Nitrogen cycling in the Middle Atlantic Bight: Results from a three-dimensional model and implications for the North Atlantic nitrogen budget, *Global Biogeochem. Cy.*, **20**, GB3007, DOI:10.1029/c2005GB002456.

Flather, R.A.(1976): A tidal model of the northwest European continental shelf, *Memoires de la Societe Royale des Sciences de Liege*, **6**(10), 141–164.

Franco, P. (1989): The northern Adriatic Sea in stratified conditions. 1. Thermohaline and density structure, hydrochemical properties: 1983, *B. Oceanol. Teor. Appl.*, Special Issue, 41–51.

Franco, P., Jeftić, L., Malanotte Rizzoli, P., Michelato, A. and Orlić, M. (1982): Descriptive model of the northern Adriatic, *Oceanol. Acta*, **5**(3), 379–389.

Haidvogel, D.B., Arango, H., Budgell, W.P., Cornuelle, B.D., Curchitser, E., Di Lorenzo, E., Fennel, K., Geyer, W.R., Hermann, A.J., Lanerolle, L., Levin, J., McWilliams, J.C., Miller, A.J., Moore, A.M., Powell, T.M., Shchepetkin, A.F., Sherwood, C.R., Signell, R.P., Warner J.C. and Wilkin, J. (2008): Ocean forecasting in terrain-following coordinates: Formulation and skill assessment of the Regional Ocean Modeling System, *J. Comput. Phys.*, **227**, 3595–3624.

Hopkins, T. S., Kinder, C., Artegiani, A. and Pariante, R. (1999): A discussion of the northern Adriatic circulation and flushing as determined from the ELNA hydrography, in *The Adriatic Sea. Ecosystem Report*, edited by T. S. Hopkins et al., *32*, European Commission, Brussels, Belgium, EUR 18834, 85–106.

Jeffries, M.A., and Lee, C.M. (2007): A climatology of the northern Adriatic Sea's response to bora and river forcing, *J. Geophys. Res*., **112**, C03S02, DOI:10.1029/2006JC003664.

Justić, D., Rabalais, N.N., Turner, R.E. and Dortch, Q. (1995): Changes in nutrient structure of river-dominated coastal waters: Stoichiometric nutrient balance and its consequences, *Estuar Coast. Shelf S.*, **40**, 339–356.

Justić, D., Bierman, V.J., Scavia, D and Hetland, R.D. (2007): Forecasting Gulf's hypoxia: next 50 years?, *Estuaries Coasts,* **30**, 791–801.

Iermano, I. (2008): La dinamica fisica e biogeochimica dell'Adriatico settentrionale investigata con simulazioni numeriche realistiche, Ph.D. Thesis, Università Politecnica delle Marche, Ancona, Italy, 172 pp. (in Italian)

Legović, T. and Justić, D. (1997): When do phytoplankton blooms cause the most intense hypoxia in the northern Adriatic Sea?, *Oceanol. Acta*, **20**(1), 91–99.

Mann, K.H and Lazier, J.R.N (1991): *Dynamics of Marine Ecosystems*. Blackwell Scientific Publications, Cambridge, 466 pp.

Martin, P.J., Book, J.W. and Doyle, J.D. (2006): Simulation of the northern Adriatic circulation during winter 2003, *J. Geophys. Res*., **111**, C03S12, DOI:10.1029/2006JC003511.

Marchesiello, P., McWilliams, J.C. and Shchepetkin, A. (2001): Open boundary conditions for long-term integration of regional oceanic models, *Ocean Model.*, **3**, 1–20.

Margolin, L. and Smolarkiewicz, P.K. (1998): Antidiffusive velocities for multipass donor cell advection, SIAM *J. Sci. Comput*., 907–929.

MEDAR Group (2002): MEDATLAS/2002 database. Mediterranean and Black Sea database of temperature salinity and bio-chemical parameters. Climatological Atlas. IFREMER Edition (4 Cdroms).

Mellor, G.L. and Yamada, T. (1982): Development of a turbulence closure model for geophysical fluid problems, *Rev. Geophys. Space Phys.*, **20**, 851–875.

Moodley, L., Heip, C.H.R. and Middelburg, J.J. (1998): Benthic activity in sediments of the northwestern Adriatic Sea: sediment oxygen consumption, macro- and meiofauna dynamics, *J. Sea Res.,* **40**, 263–280.

Murphy, A.H. (1992): Climatology, persistence, and their linear combination as standards of reference in skill scores, *Weather Forecast.*, **7**, 692–698.

Oddo, P., Pinardi, N., Zavatarelli, M. and Coluccelli, A. (2006): The Adriatic basin forecasting system, *Acta Adriatica*., **47** (Suppl.), 169–184.

Oke, P.R., Allen, J.S., Miller, R.N., Egbert, G.D., Austin, J.A., Barth, J.A., Boyd, T.J., Kosro, P.M. and Levine, M.D. (2002): A modeling study of the three-dimensional continental shelf circulation off Oregon. Part I: Model–data comparisons, *J. Phys. Oceanogr.*, **32**, 1360–1382.

Orel, G., Vio, E., Princi, M., Del Piero, D. and Aleffi, F. (1986): Stati di anossia dei fondali, popolamenti bentonici e pesca, *Nova Thalassia*, **8**, Suppl. 3, 267–280.

Orel, G., Fonda Umani, S. and Aleffi, F. (Eds.) (1993): *Ipossie e anossie di fondali marini. L'Alto Adriatico e il Golfo di Trieste*, Regione autonoma Friuli Venezia Giulia, Direzione regionale dell'Ambiente, Trieste, Italy. (in Italian).

Orlić, M., Gačić, M. and La Violette, P.E. (1992): The currents and circulation of the Adriatic Sea, *Oceanol. Acta*, **15**(2), 109–124.

Pinardi, N., Allen, I., Demirov, E., De Mey, P., Korres, G., Lascaratos, A., Le Traon, P.-Y., Maillard, C., Manzella, G., and Tziavos, C. (2003): The Mediterranean Ocean Forecasting System: first phase of implementation (1998–2001), *Ann. Geophys*. **21**, 3–20.

Poulain, P.-M. and Cushman-Roisin, B. (2001): Circulation, in *Physical Oceanography of the Adriatic Sea*, edited by B. Cushman-Roisin et al., Kluwer Academic Publishers, Dordrecht, Netherlands, 67–109.

Poulain, P.-M. and F. Raicich (2001): Forcings, in *Physical Oceanography of the Adriatic Sea*, edited by B. Cushman-Roisin et al.,, Kluwer Academic Publishers, Dordrecht, Netherlands, 45–65 pp.

Poulain, P.-M., Kourafalou, V.H., and Cushman-Roisin, B. (2001): Northern Adriatic Sea, in *Physical Oceanography of the Adriatic Sea*, edited by B. Cushman-Roisin et al., Kluwer Academic Publishers, Dordrecht, Netherlands, 143–165.

Rabalais, N.N., Turner, R.E., Justić, D., Dortch, Q. and Wiseman Jr., W.J. (1999): Characterization of hypoxia: Topic 1 Report for the integrated assessment on hypoxia in the Gulf of Mexico, NOAA Coastal Ocean Program, Silver Spring, MD, USA, 167 pp.

Raicich, F. (1994): Note on the flow rates of the Adriatic rivers. Tech. Rep. RF 02/94, 8 pp., CNR. Ist. Sper. Talassografico, Trieste, Italy.

Redfield, A.C., Ketchum, B.H. and Richards, F.A. (1974): *The influence of organisms on the composition of sea-water*, in The Sea, vol. 2, edited by M. N. Hill, Interscience, New York, 26–77.

Richards, F. A. (1965): *Anoxic basins and fjords*, in Chemical Oceanography, vol. 1, edited by J. P. Riley and G. Skirrow, Academic Press, London, 611–645.

Russo, A. and Artegiani, A. (1996): Adriatic Sea hydrography, *Sci. Mar.*, **60**, Suppl. 2, 33–43.

Russo, A., Rabitti, S. and Bastianini, M. (2002): Decadal climatic anomalies in the northern Adriatic Sea inferred from a new oceanographic data set, *Mar. Ecol.*, **23**, Suppl. 1, 340–351.

Shchepetkin, A.F. and McWilliams, J.C. (2003): A method for computing horizontal pressure-gradient force in an oceanic model with a non-aligned vertical coordinate, *J. Geophys. Res.*, **108**(C3), n. 3090, DOI:10.1029/2001JC001047.

Shchepetkin, A.F. and McWilliams, J.C. (2005), The Regional Ocean Modelling System: A split-explicit, free-surface, topography-following-coordinate oceanic model, *Ocean Model.*, **9**, 347–404.

Šimunović, A., Piccinetti, C. and Zore-Armanda, M. (1999): Kill of benthic organisms as a response to anoxic state in the northern Adriatic (a critical review), *Acta Adriatica*, **40**(1), 37–47.

Soetaert, K., Middelburg, J.J., Herman, P.M.J. and Buis, K. (2000): On the coupling of benthic and pelagic biogeochemical models, *Earth Sci. Rev.*, **51**, 173–201.

Stachowitsch, M. (1986): The Gulf of Trieste: a sensitive ecosystem, *Nova Thalassia*, **8**, Suppl. 3, 221–235.

Steppeler, J., Doms, G., Shatter, U., Bitzer, H.W., Gassmann, A., Damrath, U. and Gregoric, G. (2003): Meso-gamma scale forecasts using the nonhydrostatic model LM, *Meteorol. Atmos. Phys.*, **82**, 75–96.

Tonani, M., Pinardi, N., Dobricic, S., Pujol, I. and Fratianni, C. (2008): A high-resolution free-surface model of the Mediterranean Sea, *Ocean Sci.*, **4**, 1–14.

Ursella, L., Poulain, P.-M. and Signell, R.P. (2006): Surface drifter derived circulation in the northern and middle Adriatic Sea: Response to wind regime and season, *J. Geophys. Res.*, **111**, C03S04, DOI:10.1029/2005JC003177.

Vichi, M., Pinardi, N. and Masina, S. (2007): A generalized model of pelagic biogeochemistry for the global ocean ecosystem. Part I: Theory, *J. Marine Sys.*, **64**, 89–109.

Vilibić, I. and Supić, N. (2005): Dense water generation on a shelf: the case of the Adriatic Sea, *Ocean Dynam.*, **55**, 403–415.

Vollenweider, R.A., Marchetti, R. and Viviani, R. (eds) (1992): *Marine Coastal Eutrophication*. Elsevier, Amsterdam, 581 pp.

Wilkin, J.H. (2006): The summertime heat budget and circulation of Southeast New England shelf waters, *J. Phys. Oceanogr.*, **36**, 1997–2001.

Wu, R.S.S. (2002): Hypoxia: from molecular responses to ecosystem responses, *Mar. Pollut. Bull.*, **45**, 35–45.

Zavatarelli, M., Raicich, F., Bregant, D., Russo, A. and Artegiani, A. (1998): Climatological biogeochemical characteristics of the Adriatic Sea, *J. Marine Sys.*, **18**, 227–263.

Zore-Armanda, M. (1956): On gradient currents in the Adriatic Sea, *Acta Adriatica.*, **8**(6), 1–38.

SAŽETAK

Operativni sustav za prognoziranje hipoksije u sjevernom Jadranu

A. Russo, A. Coluccelli, I. Iermano, F. Falcieri, M. Ravaioli, G. Bortoluzzi, P. Focaccia, G. Stanghellini, C.R. Ferrari, J. Chiggiato i M. Deserti

Sjeverni Jadran (NA), najsjeverniji dio Sredozemnog mora, pod utjecajem je jakog antropogenog djelovanja (poput turizma, ribarenja, morskog prometa, istjecanje onečišćujućih tvari u poljoprivredi i industriji) te dodatno, velikog dotoka rijeka. Posljedično, djelovanje na NA ekosustav potiče ili pojačava uzdizanje sluzavih nakupina, štetno cvjetanje algi, eutrofikaciju pa čak i događaje anoksije/hipoksije. Ovaj se rad fokusira na anoksiju/hipoksiju. Tijekom ljetno-jesenskog razdoblja, NA je često izložen ovim događajima, koji se mogu kategorizirati kao obalni (relativno učestali južno od delte rijeke Po ljeti) ili udaljeni od obale (rijetki, zahvaćajući šira područja). Kako bi poboljšali poznavanje tih procesa te zbog potreba lokalne uprave, uspostavljen je operativni sustav za praćenje i prognoziranje anoksije i hipoksije u okviru EU LIFE "EMMA" projekta. Sustav se sastoji od meteorološko-oceanografske plutače; sustava za numeričku prognozu, koji se temelji na regionalnom oceanografskom modelu (ROMS), uključujući modul Fasham-tipa za biogeokemijske tokove; i periodičnim oceanografskim istraživanjima. Svakog dana, počev od lipnja 2007, sustav omogućava 3-satne prognoze morskih struja te termohalina i biogeokemijska polja za sljedeća tri dana. Sustav se pokazao sposobnim za davanje točnih prognoza temperature i relativno dobrih prognoza saliniteta i otopljenog kisika. Korijen srednje kvadratne pogreške

prognoziranog otopljenog kisika postojao je uglavnom zbog srednje pristranosti (biasa). Sustav je trenutno poboljšan tako da uključuje bolji prikaz biogeokemijskih procesa u području sloja bentosa i nekoliko prilagodba modela. Tijekom poboljšavanja modela, uklanjanjem 10-dnevne srednje pristranosti (biasa) poboljšane su prognoze otopljenog kisika.

Ključne riječi: anoksija, hipoksija, operativni model, biogeokemijski tokovi, Jadran, ROMS, oceanografska prognoza

Corresponding author's address: A. Russo, Polytechnic University of Marche – Dept. of Marine Science, Ancona, Italy, tel.: +39 071 220 433, fax.; +39 071 220 4650, e-mail: a.russo@univpm.it